HHS Public Access

Author manuscript

Adv Exp Med Biol. Author manuscript; available in PMC 2016 February 09.

Published in final edited form as:

Adv Exp Med Biol. 2016 ; 876: 185–193. doi:10.1007/978-1-4939-3023-4_23.

Approaching oxygen-guided intensity-modulated radiation therapy

Boris Epel[a,b], **Gage Redler**[a,b], **Charles Pelizzari**[a,b], **Victor M. Tormyshev**[a,c], and **Howard J. Halpern**[a,b]

[a]Center for EPR Imaging In Vivo Physiology, University of Chicago, USA

[b]Department of Radiation and Cellular Oncology, University of Chicago, USA

[c]Novosibirsk Institute of Organic Chemistry, Novosibirsk, Russia

Abstract

The outcome of cancer radiation treatment is strongly correlated with tumor oxygenation. The aim of this study is to use oxygen tension distributions in tumors obtained using Electron Paramagnetic Resonance (EPR) imaging to devise better tumor radiation treatment. The proposed radiation plan is delivered in two steps. In the first step, a uniform 50% tumor control dose (TCD_{50}) is delivered to the whole tumor. For the second step an additional dose boost is delivered to radioresistant, hypoxic tumor regions. FSa fibrosarcomas grown in the gastrocnemius of the legs of C3H mice were used. Oxygen tension images were obtained using a 250 MHz pulse imager and injectable partially deuterated trityl OX63 (OX71) spin probe. Radiation was delivered with a novel animal intensity modulated radiation therapy (IMRT) XRAD225Cx microCT/radiation therapy delivery system. In a simplified scheme for boost dose delivery, the boost area is approximated by a sphere, whose radius and position are determined using an EPR O_2 image. The sphere that irradiates the largest fraction of hypoxic voxels in the tumor was chosen using an algorithm based on Receiver Operator Characteristic (ROC) analysis. We used the fraction of irradiated hypoxic volume as the true positive determinant and the fraction of irradiated normoxic volume as the false positive determinant in the terms of that analysis. The most efficient treatment is the one that demonstrates the shortest distance from the ROC curve to the upper left corner of the ROC plot. The boost dose corresponds to the difference between TCD_{90} and TCD_{50} values. For the control experiment an identical radiation dose to the normoxic tumor area is delivered.

Keywords

Radiation therapy; oxygen guided therapy; oxygen imaging; EPR imaging

Corresponding authors Boris Epel, PhD, Center for EPR Imaging In Vivo Physiology, The University of Chicago Medical Center, Department of Radiation & Cellular Oncology, 5841 S. Maryland Ave, MC1105, room E-SB-05, Chicago, IL 60637-1463, USA, bepel@uchicago.edu. Howard J. Halpern, PhD, Center for EPR Imaging In Vivo Physiology, The University of Chicago Medical Center, Department of Radiation & Cellular Oncology, 5841 S. Maryland Ave, MC1105, room E-SB-05, Chicago, IL 60637-1463, USA, h-halpern@uchicago.edu.

1 Introduction

Common radiation delivery protocols used in cancer treatment deliver homogeneous radiation dose to a tumor [1]. This ensures destruction of cancerous cells but does not take into account different radioresistance in different portions of a tumor. It is known that tumors treated to a uniform 50% tumor control dose (TCD_{50}) exhibit different control probability depending on their oxygenation (Fig. 1) [2]. Hypoxia desensitizes tumors to radiation and mandate higher treatment doses. Knowledge of the spatial distributions of radioresistant tumor portions in combination with Intensity-Modulated Radiation Therapy (IMRT) may be used for targeted destruction of radiation-resistant areas (and sparing healthy tissues, dose painting) [3]. We expect partial oxygen pressure (pO_2) in tumor portions to be an excellent targeting parameter. This article describes the design of the experiment for the validation of oxygen-guided IMRT on mice.

2 Methods

2.1 Experiment

Figure 2 presents the flow chart of the experiment. FSa fibrosarcomas grown in the gastrocnemius of the legs of C3H mice were used. Ten-minute pO_2 images were obtained using a 250 MHz pulse EPR imager (Fig. 3A) [4] and injectable partially deuterated trityl OX63 (OX71) spin probe synthesized by the Novosibirsk Institute of Organic Chemistry. A spin-lattice relaxation based oxygen imaging protocol was used [5]. For tumor definition, an anatomic MRI image was taken prior to oxygen image. EPR and MRI images were registered with the help of fiducials embedded into a vinyl polysiloxane dental mold [6]. The ArbuzGUI MATLAB toolbox developed by the Center for EPR Imaging in vivo Physiology at the University of Chicago was used for image registration. For administration of radiation treatment an XRAD225Cx micro-CT/therapy delivery system (Figs. 3B and 4A) was used. For the first radiation treatment step, a uniform irradiation of the whole tumor to a 50% control dose (TCD_{50}) dose of 33.8 Gy was used. This dose was delivered using two opposed beams that cover the whole tumor in anterior-posterior, posterior-anterior alignments. Then a boost dose corresponding to the difference between TCD_{90} and TCD_{50} was delivered to hypoxic areas (see Sections 2.2 and 2.3). The boost dose was delivered by a 360 degree arc beam. To target the IMRT boost, a CT image was taken. Using similar fiducial technology the CT was registered to EPR image. Then the coordinates of the boost dose were transferred from the EPR to the CT image.

Animal experiments followed USPHS policy, and were approved by the Institutional Animal Care and Use Committee.

2.2 Boost dose definition algorithm

For boost dose delivery we devised a simplified scheme, where the boost volume is approximated by a sphere. The XRAD225Cx has a single beam treatment capability with 1 mm resolution. The delivery of arbitrary radiation pattern with this resolution is a very lengthy procedure. Mouse tumors models that we treat have a diameter of about 8 mm and

exhibit a very heterogeneous oxygen environment (Fig. 5A). In most cases the core of the tumor is very hypoxic and can be approximated by a sphere (Fig. 5B).

From possible positions of the radiation boost sphere, we choose the one that irradiates the largest fraction of hypoxic voxels in the tumor pO_2 image, while minimizing exposure of well-oxygenated voxels. Voxels with the oxygen tension below 10 torr were considered hypoxic, voxels above that threshold – well oxygenated. The sphere radius was chosen using an algorithm based on Receiver Operator Characteristic (ROC) analysis [7]. We used the fraction of irradiated hypoxic volume as the true positive fraction and the fraction of irradiated normoxic volume as the false positive fraction in the terms of that analysis (Fig. 6). The most efficient treatment is the one that demonstrates the shortest distance from the ROC curve to the upper left corner of the plot (Fig. 6). For the control experiment an identical radiation dose to the normoxic tumor area is delivered.

The control scheme for validation of the proposed method efficiency includes radiation delivery to tumor or normal tissue of equal volume, where the hypoxic areas of the tumor are avoided by delivering a shell-shaped radiation dose to well-oxygenated areas equal to the boost dose. The collimator used for anti-boost delivery is presented in Figs. 4B and 4C. It consists of two coaxial elements: one with a circular opening and circular radiation blocker (Fig. 4C). The cross-sections of radiation beam for boost and anti-boost therapies are shown in the Figure 5B.

2.3 Radiation dose calculation and verification

Radiation planning used an open-source treatment planning system developed in MATLAB, which was provided by Precision X-ray (North Branford, CT, USA). The software allows identification of a target point and treatment volume on a mouse cone-beam CT (CBCT) scan taken with the animal immobilized in the treatment position after it has been transferred from the EPRI O_2 imager to the treatment machine. The user can select from a set of available beam sizes (normally cylindrical, though this is not a requirement) and choose a set of incident directions, which may be discrete angles or continuous arcs, all parallel to the transverse CBCT plane, i.e., normal to the inferior-superior axis of the animal. Given a user-specified dose per beam, previously acquired calibration dosimetry data are used to compute the integrated exposure in milliamp-seconds required for each discrete field or arc. A radiation protocol is saved on the instrument control PC which is read in by the XRad225Cx control software to automatically deliver the specified beams, sequencing from one beam or arc to the next and turning the X-ray beam on and off for the required time and beam current.

Dose distributions are verified using Monte Carlo calculations performed offline. The calculations were too long to be carried during the oxygen targeting protocol. The EGSnrc system from the National Research Council Canada [8] is used for these calculations. A model of the XRad225Cx treatment head including the Comet MXR-225/22 X-ray tube, primary collimator, aluminum and copper filters, and treatment apertures (cones) for each available radiation field size have been built using the BEAMnrc user code. For each field size and beam quality, a phase space file is computed which summarizes the energy, spatial and orientation distribution of radiation crossing the aperture exit. Histories of 500 million

to 1 billion incident electrons are used to generate each phase space file. These pre-computed phase space files are then used in the DOSXYZnrc user code [9] to simulate radiation transport and dose deposition through the case-specific animal geometry derived from the pretreatment CBCT [10] used for treatment planning. Dose is typically accumulated on a 3D, isotropic 0.2 mm grid for 100-500 million X-ray histories incident from the phase space plane. Results can be superimposed in 3D with the CBCT image, which is in the same coordinate system, as illustrated in Fig. 7. Any other image volume registered with the CBCT, in particular the EPR oxygen map, can also be superimposed with the Monte Carlo generated dose distribution for display and analysis.

3 Discussion

The delivery of the oxygen-guided radiotherapy to small rodents presents a substantial technological challenge. The typical size of tumors in our studies is about 8 mm in diameter. To achieve spatial localization of treatment not worse than 15% of tumor diameter, all stages of the protocol have to exhibit better than 1 mm precision. The resolution of CT and MRI images are considerably higher than 1 mm. The resolution of the EPR image is about 1.2 mm. However, the fiducial image used for image registration is acquired in higher resolution (0.66 mm). According to our experience, the registration procedure for tumor bearing leg gives a precision comparable with the resolution of the lowest resolved image, about 0.6 mm. The leg tumor is not susceptible to breathing motion artifacts and its position is well preserved by the vinyl polysiloxane cast during the whole imaging and treatment protocol. Finally, the spatial resolution of the radiation delivery system, considering beam penumbra and the interaction of the radiation beam with tissues and other materials in the radiation window, is estimated to be ~ 1 mm. Thus the overall spatial resolution of the oxygen guided intensity-modulated radiation therapy is about 1 mm. This resolution appears to be consistent with our results demonstrating correlation between the outcome of radiation therapy and tissue oxygenation in tumors [2].

4 Conclusions

This work presents the first practical implementation of EPR oxygen image-guided radiation therapy. The experiments determining the outcome of the proposed scheme are currently underway.

Acknowledgments

Supported by NIH grants P41 EB002034 and R01 CA98575. Monte Carlo computations are performed on a computer cluster administered by the Department of Radiology and partially supported by the University of Chicago Comprehensive Cancer Center (NCI P30 CA014599).

References

1. Khan, FM. Fourth. Lippincott Williams & Wilkins; 2010. The Physics of Radiation Therapy.
2. Elas M, Magwood JM, Butler B, et al. EPR Oxygen Images Predict Tumor Control by a 50% Tumor Control Radiation Dose. Cancer Res. 2013; 73:5328–5335. [PubMed: 23861469]
3. Ling CC, Humm J, Larson S, et al. Towards multidimensional radiotherapy (MD-CRT): Biological imaging and biological conformality. Int J Radiat Oncolo Biol Physics. 2000; 47:551–560.

4. Epel B, Sundramoorthy SV, Mailer C, et al. A versatile high speed 250-MHz pulse imager for biomedical applications. Conc Magn Reson B. 2008; 33B:163–176.
5. Epel B, Bowman MK, Mailer C, et al. Absolute oxygen R_{1e} imaging in vivo with pulse electron paramagnetic resonance. Magnet Reson Med. 2013 (eprint ahead of pub).
6. Haney CR, Fan X, Parasca AD, et al. Immobilization using dental material casts facilitates accurate serial and multimodality small animal imaging. Conc Magn Reson B. 2008; 33B:138–144.
7. Metz CE. Basic Principles of Roc Analysis. Semin Nucl Med. 1978; 8:283–298. [PubMed: 112681]
8. Kawrakow I. Accurate condensed history Monte Carlo simulation of electron transport. I. EGSnrc, the new EGS4 version. Med Physics. 2000; 27:485–498.
9. Kawrakow I, Walters BRB. Efficient photon beam dose calculations using DOSXYZnrc with BEAMnrc. Med Physics. 2006; 33:3046–3056.
10. Rogers DWO, Faddegon BA, Ding GX, et al. Beam - a Monte-Carlo Code to Simulate Radiotherapy Treatment Units. Med Physics. 1995; 22:503–524.

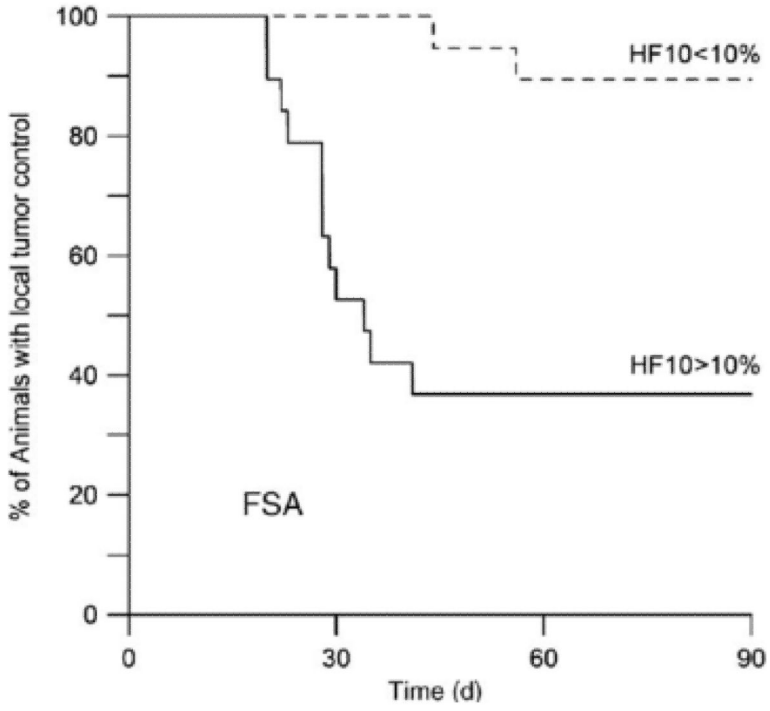

Fig. 1.

Kaplan-Meier plot showing the percentage of animals with local tumor control as a function of time after treatment with a single TCD50 dose (33.8 Gy) of X-rays [2]. Hypoxic fraction of voxels below 10% (HF10) was used for analysis. FSa fibrosarcoma tumor mode was used.

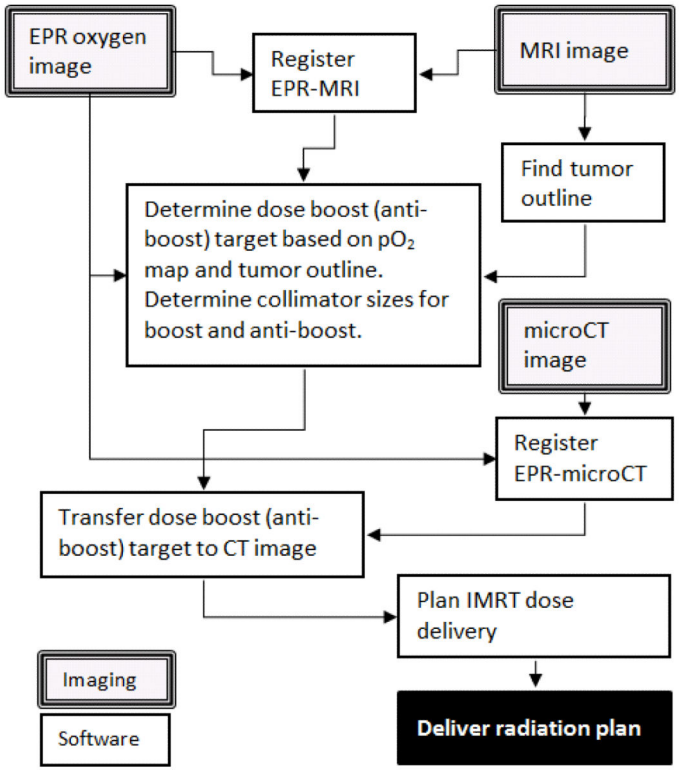

Fig. 2.
Flow chart of the treatment protocol.

Fig. 3.

A. 250 MHz pulse Electron Paramagnetic Resonance oxygen imager. **B**. Precision X-ray XRAD225Cx image-guided biologic irradiator/CT imager.

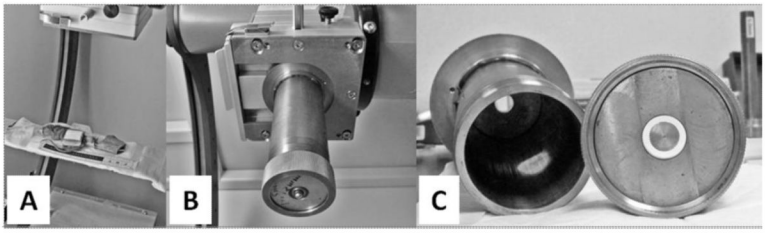

Fig. 4.

Irradiation setup. **A**. Animal placed on the animal support. **B**. Irradiation of head with the collimator installed. **C**. Collimator set-up for anti-boost treatment protocol. The diaphragm consists of two concentric lead elements to deliver shell-shaped radiation dose.

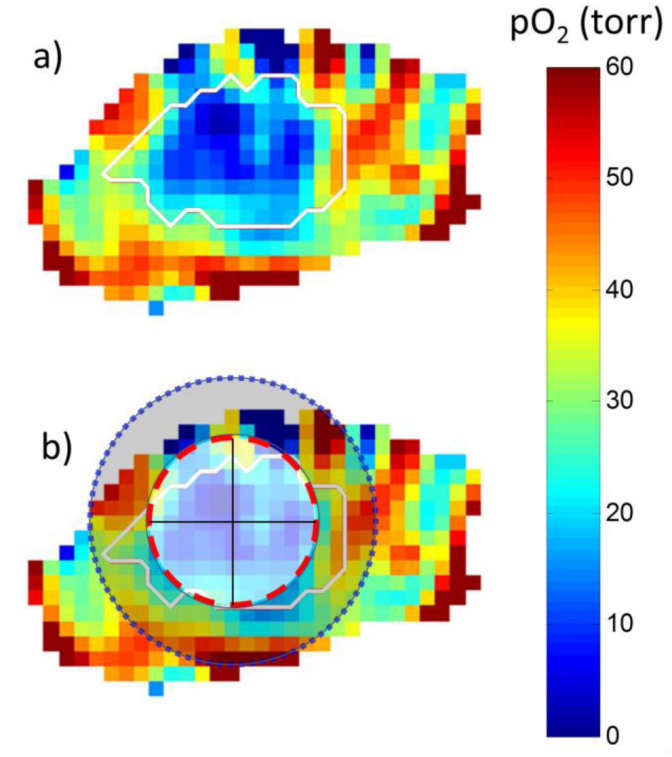

Fig. 5.

EPR oxygen image of the leg tumor. **A.** Oxygen map with tumor contour transferred from the registered MRI image. **B.** Boost (red line) and anti-boost (shaded area) as determined by the boost planning software.

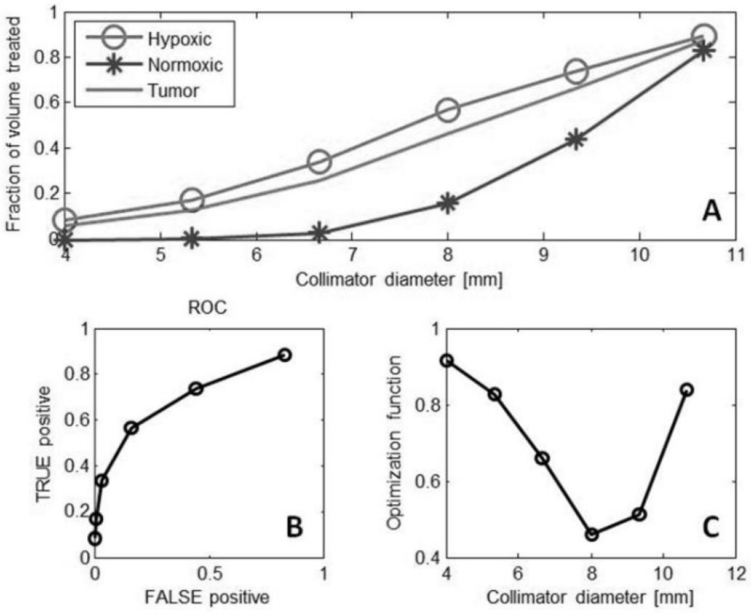

Fig. 6.

Dose boost planning algorithm for both hypoxic region targeting and hypoxic region avoidance. (**A**) EPROI of an FSa fibrosarcoma tumor implanted and grown on a mouse leg. The white outline shows the tumor outline from registered MRI. (**B**) Same EPROI with the spherical hypoxic boost region (lightened dash red outline) and spherical shell anti-boost region (darker ring/blue dot outline).

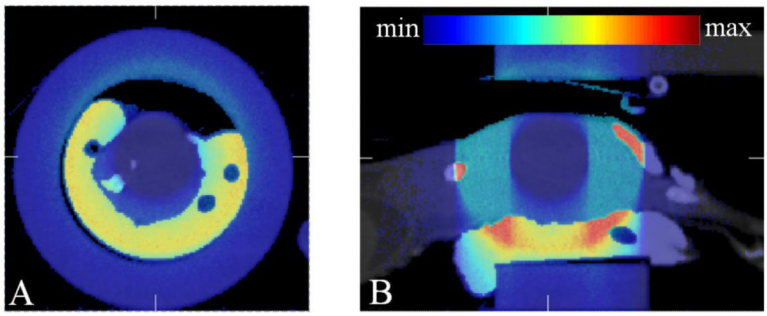

Fig. 7.

Axial and sagittal views of the anti-boost dose intensity profile as obtained from Monte Carlo calculations. The dose is delivered using a 360 degree arc turn of the irradiation head located in the plane perpendicular to the plane of the left panel. The EGSnrc system from the National Research Council of Canada was used for calculations.